

# UC Santa Barbara

## UC Santa Barbara Previously Published Works

**Title**

Effect of postdeposition anneals on the Fermi level response of HfO<sub>2</sub>/In<sub>0.53</sub>Ga<sub>0.47</sub>As gate stacks

**Permalink**

<https://escholarship.org/uc/item/38d8t95j>

**Journal**

Journal of Applied Physics, 108(3)

**Author**

Stemmer, Susanne

**Publication Date**

2010

**DOI**

10.1063/1.3465524

Peer reviewed

# Effect of postdeposition anneals on the Fermi level response of $\text{HfO}_2/\text{In}_{0.53}\text{Ga}_{0.47}\text{As}$ gate stacks

Yoontae Hwang, Roman Engel-Herbert, Nicholas G. Rudawski, and Susanne Stemmer<sup>a)</sup>  
Materials Department, University of California, Santa Barbara, California 93106-5050, USA

(Received 30 May 2010; accepted 17 June 2010; published online 10 August 2010)

The electrical characteristics, in particular interface trap densities, oxide capacitance, and Fermi level movement, of metal oxide semiconductor capacitors with  $\text{HfO}_2$  gate dielectrics and  $\text{In}_{0.53}\text{Ga}_{0.47}\text{As}$  channels are investigated as a function of postdeposition annealing atmosphere. It is shown, using both conductance and Terman methods, that the Fermi level of nitrogen annealed stacks is effectively pinned at midgap. In contrast, samples annealed in forming gas show a large band bending in response to an applied gate voltage and a reduced midgap interface trap density compared to those annealed in nitrogen. © 2010 American Institute of Physics.  
[doi:10.1063/1.3465524]

## I. INTRODUCTION

The development of metal oxide semiconductor field effect transistors with high-mobility III-V semiconductor channels faces considerable challenges because of the high trap densities ( $D_{it}$ ) at the oxide/semiconductor interface, which cause Fermi level pinning. The high  $D_{it}$  appears to be a general property of these interfaces, independent of the specific high-permittivity ( $k$ ) dielectric.<sup>1-4</sup> The reasons for the high  $D_{it}$  are presently not understood, although it has been suggested that they may be an intrinsic property of a defective III-V surface.<sup>5-7</sup> For interfaces with  $\text{In}_{0.53}\text{Ga}_{0.47}\text{As}$  the typical  $D_{it}$  distribution in the band gap results in electrical characteristics that have been described as “weak Fermi level pinning,”<sup>8</sup> i.e., the Fermi level can be moved over some range within the band gap. In this case, changing the gate voltage results in nonzero band bending for all applied gate voltages; however, a large midgap  $D_{it}$  combined with an insufficient oxide capacitance usually prevents moving the Fermi level into the lower half of the band gap (for  $n$ -type channels) at practical oxide thicknesses even for the largest applied negative gate voltage. Such interfaces are described in the following as “effectively pinned at midgap.” Recently, several approaches have been reported that potentially can serve to reduce the  $D_{it}$ , including sulfur passivation<sup>3,9</sup> and hydrogen annealing.<sup>10,11</sup> In particular, for  $\text{Al}_2\text{O}_3/\text{III-V}$  interfaces, forming gas anneals (which contain a few percent hydrogen) have resulted in significant improvements in the capacitance-voltage (CV) characteristics, with reduced interface trap response at negative gate biases for  $n$ -type channels and a lowering of the frequency dispersion in accumulation.<sup>10,11</sup>

In this paper we show that forming gas anneals can reduce the midgap- $D_{it}$  of  $\text{HfO}_2/\text{In}_{0.53}\text{Ga}_{0.47}\text{As}$  interfaces to a sufficiently low level that—in conjunction with a low equivalent oxide thicknesses (EOT)—the Fermi level can be moved across midgap. Evidence for an unpinned Fermi level is provided by a large semiconductor band bending deep into

the semiconductor band gap and by efficient movement of parallel conductance peaks. The characteristics of the forming gas annealed gate stacks are contrasted with those of a pinned  $\text{HfO}_2/\text{In}_{0.53}\text{Ga}_{0.47}\text{As}$  interface annealed in nitrogen.

## II. EXPERIMENTAL

Substrates were commercial, As-capped,  $n$ -type Si-doped ( $1 \times 10^{17} \text{ cm}^{-3}$ )  $\text{In}_{0.53}\text{Ga}_{0.47}\text{As}$  films with a thickness of 300 nm grown by molecular beam epitaxy (MBE) lattice-matched on  $n^+$  (001) InP wafers (IntelliEpi, Richardson, Texas). Before  $\text{HfO}_2$  growth in a MBE system, the As-cap was removed *in situ* by heating until a streaky ( $2 \times 4$ ) surface reconstruction was obtained in reflection high-energy electron diffraction. The surface was then exposed to a flux of trimethylaluminum (TMA) for 30 s at a substrate temperature of 300 °C. The sample temperature was raised to 400 °C and  $\text{HfO}_2$  was deposited using hafnium tert-butoxide as the source, as described elsewhere.<sup>2</sup> The TMA acted as a surfactant and allowed for the growth of thin, coalesced and smooth  $\text{HfO}_2$  films. Without TMA dosing of the  $\text{In}_{0.53}\text{Ga}_{0.47}\text{As}$  surface,  $\text{HfO}_2$  films grew in an island mode and were not coalesced until about 30 nm thickness.<sup>2</sup> Transmission electron microscopy imaging and diffraction showed that the as-deposited  $\text{HfO}_2$  films were crystalline and contained a mixture of monoclinic and tetragonal grains. The tetragonal phase can be stabilized by incorporation of Al, such as from the TMA dosing.<sup>12</sup> Metal-oxide-semiconductor capacitor (MOSCAP) structures were fabricated with 50 nm thick Pt metal gates (area  $A = 1.77 \times 10^{-4} \text{ cm}^2$ ) by electron beam evaporation through a shadow mask and annealed in forming gas (95% of  $\text{N}_2$  and 5% of  $\text{H}_2$ ) for 50 min at 400 °C. A control sample was annealed immediately after deposition for 30 min at 300 °C in nitrogen. This sample was not annealed in forming gas. Back Ohmic contacts were Ti (20 nm)/Pt (20 nm)/Au (250 nm) that were In-bonded to an Au-coated sapphire wafer. Frequency-dependent CV and conductance-voltage measurements were performed at room temperature from 1 kHz to 1 MHz in the dark using an impedance analyzer (Agilent 4294). Capacitance and conduc-

<sup>a)</sup>Electronic mail: stemmer@mrl.ucsb.edu.

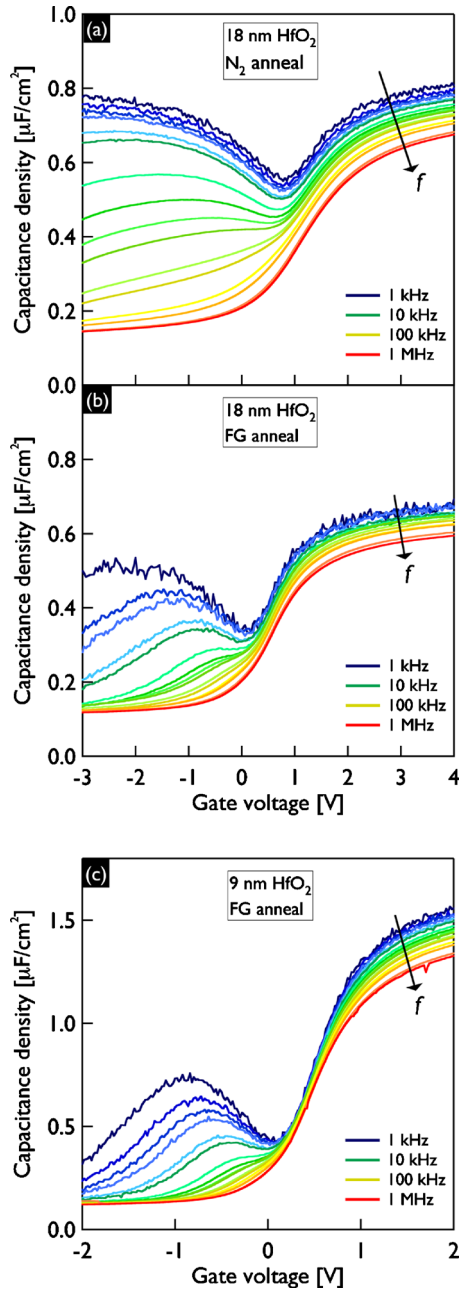


FIG. 1. (Color online) Frequency-dependent CV characteristics of  $\text{HfO}_2/n$ -type  $\text{In}_{0.53}\text{Ga}_{0.47}\text{As}$  MOSCAPs at 300 K: (a) 18 nm  $\text{HfO}_2$ , nitrogen annealed (b) 18 nm  $\text{HfO}_2$ , forming gas (FG) annealed, and (c) 9 nm  $\text{HfO}_2$ , forming gas annealed.

tance values were corrected for series resistance (Eqs. 5.88, 5.90, and 5.91 in Ref. 13).

### III. RESULTS AND DISCUSSION

Figure 1 shows the CV characteristics of nitrogen [Fig. 1(a)] and forming gas annealed stacks [Figs. 1(b) and 1(c)], respectively. For the forming gas annealed stacks, results for two different  $\text{HfO}_2$  thicknesses,  $\sim 18$  nm [Fig. 1(b)] and  $\sim 9$  nm [Fig. 1(c)] are shown. Comparison of the CV of the nitrogen and forming gas annealed stacks already shows qualitatively that the  $D_{it}$  is reduced as a result of the forming gas anneal: (i) the frequency dispersion in depletion and accumulation and the CV stretch-out are smaller; (ii) the large

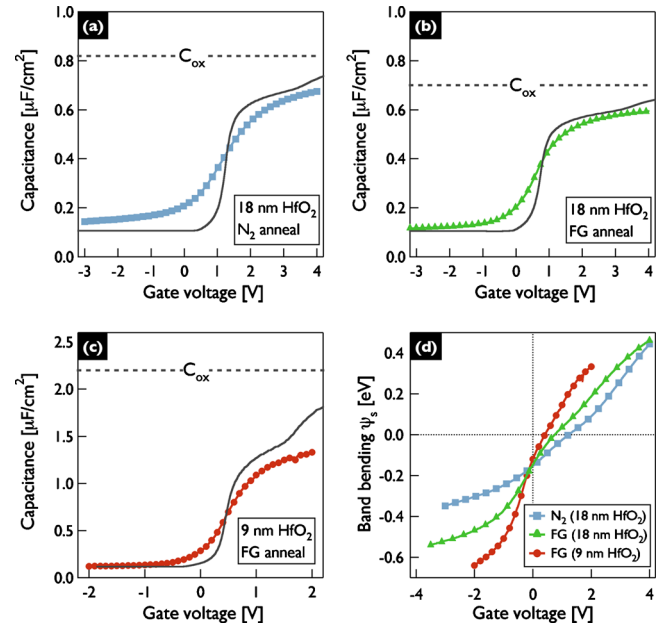


FIG. 2. (Color online) Comparison of modeled (solid black lines) and experimental (symbols) 1 MHz CV curves for the three stacks shown in Fig. 1. (a) 18 nm  $\text{HfO}_2$ , nitrogen annealed, (b) 18 nm  $\text{HfO}_2$ , forming gas annealed, and (c) 9 nm  $\text{HfO}_2$ , forming gas annealed. (d) Band bending  $\psi_s$  as a function of gate voltage extracted from the Terman method for the three samples shown in Fig. 1. The flat band condition corresponds to  $\psi_s=0$ .

midgap  $D_{it}$  response, which is responsible for the rise in the capacitance at negative bias with decreasing frequency,<sup>2</sup> is suppressed; and (iii) the capacitance in depletion is close to its ideal value ( $0.119 \mu\text{F}/\text{cm}^2$  for a semiconductor doping of  $10^{17} \text{cm}^{-3}$ , also see Fig. 2). In contrast, the depletion capacitance is larger for the nitrogen annealed stack ( $0.144 \mu\text{F}/\text{cm}^2$ ). The larger value is an indication of Fermi level pinning around midgap, as the applied gate bias cannot fully deplete the semiconductor. Conversely, the fact that the forming gas annealed stacks reach the ideal depletion capacitance indicates efficient band bending. The CV behavior of the nitrogen annealed stack, with its large stretch-out and significant frequency dispersion at negative biases, is very similar to what has been reported for many high- $k$  oxides on  $\text{In}_{0.53}\text{Ga}_{0.47}\text{As}$  at room temperature in the literature.<sup>2,3,9,14–18</sup>

For a more quantitative analysis, Fig. 2 shows a comparison of ideal and experimental 1 MHz CV curves for all three stacks shown in Fig. 1, from which the band bending as a function of the applied gate voltage is extracted using the Terman method.<sup>13</sup> The modeled CV curve correctly accounts for the finite conduction band density of states (DOS), the nonparabolicity of the  $\Gamma$ -band and the occupation of higher lying valleys in the conduction band. Details on the CV modeling will be reported elsewhere.<sup>19</sup> The oxide capacitance density,  $C_{ox}$ , is also shown for each case, which is higher than the capacitance in accumulation because of the finite DOS in the conduction band. Mapping the experimental CV to the simulated curves yielded  $C_{ox}$  values of  $0.82$  and  $0.70 \mu\text{F}/\text{cm}^2$  for 18 nm  $\text{HfO}_2$  films after nitrogen and forming gas annealing, respectively, and  $2.2 \mu\text{F}/\text{cm}^2$  for the 9 nm  $\text{HfO}_2$  film annealed in forming gas. These capacitance densities correspond to EOT values of 4, 4.9, and 1.6 nm for the three gate stacks. This yields a dielectric constant of 22

for the 9 nm HfO<sub>2</sub>, which is higher than that of monoclinic HfO<sub>2</sub>, and is most likely due to the presence of the higher-*k* tetragonal phase<sup>20</sup> seen in electron diffraction. The dielectric constant is in excellent agreement with that estimated from a thickness series.<sup>2</sup>

The extracted band bending is shown in Fig. 2(d) for all three stacks. For the nitrogen annealed gate stack a band bending of  $-0.35$  eV is achieved at a voltage  $\Delta V = V_{FB} - V_g$  of 4.24 V, where  $V_{FB}$  is the flat band voltage and  $V_g$  the applied gate voltage. The limited band bending indicates that for the nitrogen annealed stack, the Fermi level cannot be moved past midgap for the maximum applied negative voltage and it is effectively pinned. In contrast, the forming gas annealed stacks achieve the same band bending at  $\Delta V = 1.64$  V (18 nm film) and  $\Delta V = 0.95$  V (9 nm film), respectively. For the 9 nm forming gas annealed film, the band bending exceeds half the band gap of In<sub>0.53</sub>Ga<sub>0.47</sub>As at the maximum applied negative voltage, indicating an unpinned Fermi level that is not impeded by the midgap  $D_{it}$ .

Further evidence of an unpinned Fermi level for the forming gas annealed stack and a measure of the midgap  $D_{it}$  can be obtained from conductance maps, which plot  $(G_p/\omega)/Aq$  as a function of frequency and applied gate bias, where  $q$  is the elemental charge and  $G_p/\omega$  is the parallel conductance.  $G_p/\omega$  is obtained from the measured conductance and the oxide capacitance density,  $C_{ox}$  (see Eq. 5.77 in Ref. 13). The  $D_{it}$  in depletion is estimated by multiplying the peak,  $[(G_p/\omega)/Aq]_{max}$ , with a factor of  $\sim 2.5$ .<sup>13</sup> It has been shown that the conductance method can give reliable estimates of the midgap  $D_{it}$  for high-*k*/III-V interfaces provided that the  $D_{it}$  is sufficiently low, i.e.,  $C_{ox} > qD_{it}$ .<sup>8,21</sup> Furthermore, the movement of conductance peaks in these maps is an indicator of the band bending efficiency as a function of applied bias.<sup>8</sup>

Figure 3 shows conductance maps for the 18 nm nitrogen annealed [Fig. 3(a)] and for the 9 nm forming gas annealed [Fig. 3(b)] HfO<sub>2</sub>, respectively. For the nitrogen annealed sample, the  $(G_p/\omega)/Aq$  peak responds only moderately to the applied negative gate bias (see dashed arrows), indicating inefficient band bending.<sup>8</sup> In contrast, for the forming gas annealed stack, the peak follows the gate bias efficiently, indicating that the Fermi level is unpinned between about 0.15 to 0.3 eV below the conduction band (for the alignment of the position in the band gap see Ref. 2). Consistent with Fermi level unpinning, the midgap  $D_{it}$  is lower in the forming gas annealed stack, with a peak value of  $10^{13}$  cm<sup>-2</sup> eV<sup>-1</sup>. This value is reliable, because  $C_{ox} > qD_{it}$  for this stack. In contrast, the conductance map for the nitrogen annealed film shows a  $D_{it}$  of greater than  $2.5 \times 10^{13}$  cm<sup>-2</sup> eV<sup>-1</sup>. However, this value is likely a severe underestimate of the true  $D_{it}$ , because for this stack,  $C_{ox} < qD_{it}$ .<sup>8</sup>

#### IV. CONCLUSIONS

In summary, depletion capacitance values that are close to their correct value, conductance maps, and a large band bending of more than half the band gap of In<sub>0.53</sub>Ga<sub>0.47</sub>As in response to an applied gate bias all indicate that the Fermi

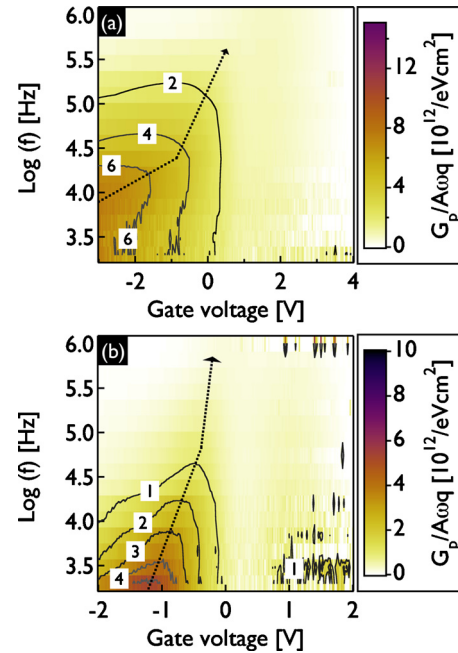


FIG. 3. (Color online) Normalized parallel conductance,  $(G_p/\omega)/Aq$ , as a function of gate voltage and frequency  $f$  measured at 300 K for (a) 18 nm HfO<sub>2</sub>, nitrogen annealed and (b) 9 nm HfO<sub>2</sub>, forming gas annealed. The scale bar on the right can be used to extract the  $(G_p/\omega)/Aq$  peak values, which are also given at the contour lines in the map. The dotted arrows are a guide to the eye to trace the position of the  $(G_p/\omega)/Aq$  maxima in the depletion region.

level of HfO<sub>2</sub>/In<sub>0.53</sub>Ga<sub>0.47</sub>As interfaces can be moved efficiently across midgap by annealing in forming gas. The Fermi level unpinning is due to a combination of a sufficiently large oxide capacitance and a sufficiently reduced  $D_{it}$  near midgap, even though the  $D_{it}$  is still high ( $10^{13}$  cm<sup>-2</sup> eV<sup>-1</sup>). Future studies should investigate the underlying physical mechanisms by which hydrogen gas containing anneals can reduce the midgap  $D_{it}$ .

#### ACKNOWLEDGMENTS

The research was funded by the Semiconductor Research Corporation through the Nonclassical CMOS Research Center (Task ID 1437.005). This work made use of the UCSB Nanofabrication Facility, a part of the NSF-funded NNIN network.

<sup>1</sup>G. Brammertz, H. C. Lin, K. Martens, D. Mercier, C. Merckling, J. Pénard, C. Adelman, S. Sioncke, W. E. Wang, M. Caymax, M. Meuris, and M. Heyns, *J. Electrochem. Soc.* **155**, H945 (2008).

<sup>2</sup>Y. Hwang, R. Engel-Herbert, N. G. Rudawski, and S. Stemmer, *Appl. Phys. Lett.* **96**, 102910 (2010).

<sup>3</sup>E. O'Connor, S. Monaghan, R. D. Long, A. O'Mahony, I. M. Povey, K. Cherkaoui, M. E. Pemble, G. Brammertz, M. Heyns, S. B. Newcomb, V. V. Afanas'ev, and P. K. Hurley, *Appl. Phys. Lett.* **94**, 102902 (2009).

<sup>4</sup>A. Ali, H. Madan, S. Kovesnikov, S. Oktyabrsky, R. Kambhampati, T. Heeg, D. Schlom, and S. Datta, *IEEE Trans. Electron Devices* **57**, 742 (2010).

<sup>5</sup>W. E. Spicer, I. Lindau, P. Skeath, C. Y. Su, and P. Chye, *Phys. Rev. Lett.* **44**, 420 (1980).

<sup>6</sup>H. Hasegawa and H. Ohno, *J. Vac. Sci. Technol. B* **4**, 1130 (1986).

<sup>7</sup>M. D. Pashley, K. W. Haberern, R. M. Feenstra, and P. D. Kirchner, *Phys. Rev. B* **48**, 4612 (1993).

<sup>8</sup>H. C. Lin, G. Brammertz, K. Martens, G. de Valicourt, L. Negre, W. E. Wang, W. Tsai, M. Meuris, and M. Heyns, *Appl. Phys. Lett.* **94**, 153508 (2009).

- (2009).
- <sup>9</sup>H. C. Lin, W. E. Wang, G. Brammertz, M. Meuris, and M. Heyns, *Microelectron. Eng.* **86**, 1554 (2009).
- <sup>10</sup>E. J. Kim, L. Q. Wang, P. M. Asbeck, K. C. Saraswat, and P. C. McIntyre, *Appl. Phys. Lett.* **96**, 012906 (2010).
- <sup>11</sup>S. Oktyabrsky, Y. Nishi, S. Kovesnikov, W.-E. Wang, N. Goel, and W. Tsai, in *Fundamentals of III-V Semiconductor MOSFETs*, edited by S. Oktyabrsky and P. D. Ye (Springer, New York, 2010).
- <sup>12</sup>Y. Yang, W. J. Zhu, T. P. Ma, and S. Stemmer, *J. Appl. Phys.* **95**, 3772 (2004).
- <sup>13</sup>E. H. Nicollian and J. R. Brews, *MOS (Metal Oxide Semiconductor) Physics and Technology* (Wiley, New York, 1982).
- <sup>14</sup>H. C. Chiu, L. T. Tung, Y. H. Chang, Y. J. Lee, C. C. Chang, J. Kwo, and M. Hong, *Appl. Phys. Lett.* **93**, 202903 (2008).
- <sup>15</sup>N. Goel, P. Majhi, W. Tsai, M. Warusawithana, D. G. Schlom, M. B. Santos, J. S. Harris, and Y. Nishi, *Appl. Phys. Lett.* **91**, 093509 (2007).
- <sup>16</sup>S. Kovesnikov, N. Goel, P. Majhi, H. Wen, M. B. Santos, S. Oktyabrsky, V. Tokranov, R. Kambhampati, R. Moore, F. Zhu, J. Lee, and W. Tsai, *Appl. Phys. Lett.* **92**, 222904 (2008).
- <sup>17</sup>E. J. Kim, E. Chagarov, J. Cagnon, Y. Yuan, A. C. Kummel, P. M. Asbeck, S. Stemmer, K. C. Saraswat, and P. C. McIntyre, *J. Appl. Phys.* **106**, 124508 (2009).
- <sup>18</sup>R. Engel-Herbert, Y. Hwang, J. Cagnon, and S. Stemmer, *Appl. Phys. Lett.* **95**, 062908 (2009).
- <sup>19</sup>R. Engel-Herbert, Y. Hwang, and S. Stemmer, "Quantification of trap densities at dielectric/III-V semiconductor interfaces," *Appl. Phys. Lett.* (2010) (to be published).
- <sup>20</sup>X. Y. Zhao and D. Vanderbilt, *Phys. Rev. B* **65**, 233106 (2002).
- <sup>21</sup>K. Martens, C. O. Chui, G. Brammertz, B. De Jaeger, D. Kuzum, M. Meuris, M. M. Heyns, T. Krishnamohan, K. Saraswat, H. E. Maes, and G. Groeseneken, *IEEE Trans. Electron Devices* **55**, 547 (2008).